Desalination and Water Treatment
www.deswater.com
doi: 10.1080/19443994.2015.1079741

57 (2016) 16583–16591
July

Taylor & Francis
Taylor & Francis Group

Vanadium removal from aqueous solutions by adsorption onto chitosan films

Tito Roberto Santana Cadaval Jr.[a,*], Guilherme Luiz Dotto[b], Elisa Rosa Seus[c], Nicolai Mirlean[c], Luiz Antonio de Almeida Pinto[a]

[a]*Unit Operations Laboratory, School of Chemistry and Food, Federal University of Rio Grande. FURG, Rio Grande, RS, Brazil, Tel. +55 53 3233 6969; emails: titoeq@gmail.com (T.R.S. Cadaval), dqmpinto@furg.br (L.A. de Almeida Pinto)*
[b]*Chemical Engineering Department, Federal University of Santa Maria, UFSM, Santa Maria, RS, Brazil, email: guilherme_dotto@yahoo.com.br*
[c]*Oceanography Institute, Federal University of Rio Grande, FURG, Rio Grande, RS, Brazil, emails: elisarosaseus@yahoo.com.br (E.R. Seus), dgeonmir@furg.br (N. Mirlean)*

Received 2 April 2015; Accepted 25 July 2015

ABSTRACT

Chitosan films (CF) are an interesting way to remove heavy metals from aqueous solutions. The effluents containing vanadium is highly toxic from environmental viewpoint, then, the aim of this work was to evaluate the vanadium adsorption onto CF. The films were prepared by casting technique and characterized (tensile strength, elongation, and thickness). The vanadium adsorption was optimized as a function of the pH and film dosage by response surface methodology. The equilibrium isotherms were obtained and the thermodynamic parameters were estimated. The vanadium–CF interactions were elucidated, and also regeneration studies were performed. The more suitable adsorption conditions were in pH 6 and film dosages of 100 and 300 mg L^{-1}, under these conditions, the vanadium removal percentage and adsorption capacity were of 50.3% and 251.4 mg g^{-1}, respectively. The BET model showed best fit for the experimental equilibrium data. The adsorption process was spontaneous, favorable, and endothermic. Fourier transform infrared spectroscopy and thermogravimetric analysis confirmed the presence of vanadium on CF after adsorption. Desorption was possible with 0.01 mol L^{-1} NH_4Cl solution. The CF maintained the structural characteristics and adsorption capacities after six cycles of regeneration.

Keywords: Adsorption capacity; Chitosan film; Equilibrium; Vanadium

1. Introduction

Several alternative adsorbents are researched to remove heavy metals from aqueous solutions, such as limonite [1], magnetite [2], *Spirulina platensis* [3], sugarcane bagasse [4], olive stone [5], and cow dung powder [6]. In this context, chitosan, a linear biopolymer of acetylamino-D-glucose, obtained from chitin alkaline deacetylation, stands out, due to its high content of amino and hydroxyl groups, which shows elevated potential for interaction with pollutants [7]. Nevertheless, when chitosan is used in powder form [7,8], the centrifugation and/or filtration are necessary for the phase separation after adsorption process [9], and desorption process is the hardest. Then, it is desirable that the development of chitosan-based materials in order to facilitate the phase separation and its regeneration.

*Corresponding author.

Among the chitosan-based materials, the chitosan film is an interesting way to remove heavy metals from aqueous solutions. The main advantages for the application of chitosan films (CF) are its good tensile strength, elongation, swelling properties, applicability to a wide range of pH, and regeneration [10–13]. Dotto et al. [9] reported that the mechanical properties of CF were maintained during the food dyes adsorption, leading to benefits for practical applications. The literature shows that CF are effective to remove lead [10], chromium [11,12], and mercury [12] from aqueous solutions.

Vanadium is a transition metal which is employed in various industrial fields, including metallurgy and nuclear reactors [14]. Significant vanadium concentrations (from 10 to 1,400 mg L^{-1}) are also found in petroleum and its derivate [15]. Combustion in thermal power plants and regeneration processes in petrochemical industries produce the effluents containing vanadium [16]. It is very difficult to remove vanadium from aqueous phase, so large volumes of water containing this metal are discarded. Furthermore, vanadium is highly toxic from environmental viewpoint [17]. Treatment techniques, such as solvent extraction, ion–exchange resins, and electrokinetic processes are used, but these are not economically viable [18]. In this way, adsorption is considered as one of the most suitable and low-cost alternative methods for pollutants removal from aqueous media [18,19].

This work aimed the vanadium removal from aqueous solutions by adsorption onto CF. The CF were prepared by casting technique and were characterized. The vanadium adsorption was optimized as a function of pH (4, 6, and 8) and CF dosage (100, 300, and 500 mg L^{-1}) by response surface methodology (RSM). The equilibrium isotherms were obtained (at 293, 313, and 333 K) and the thermodynamic parameters were estimated. The CF–vanadium interactions were elucidated by Fourier transform infrared spectroscopy (FTIR) and thermogravimetric analysis (TGA). Adsorption–desorption cycles were performed.

2. Material and methods

2.1. Preparation and characterization of CF

Chitosan (molecular weight 150 ± 3 kDa, deacetylation degree of 85 ± 1%, and mean diameter of 72 ± 3 μm) was obtained from shrimp (*Penaeus brasiliensis*) wastes by the following steps: demineralization, deproteinization, deodorization, deacetylation, purification, and drying [20–22]. The CF were produced by casting technique as following: 1.5 g of chitosan powder was dissolved in 0.1 mol L^{-1} of acetic acid solution. Then the film-forming solution was centrifuged at 5,000 ×*g* for 15 min. Film-forming solution was poured onto a level plexiglas plate. The CF were obtained by solvent evaporation in an oven with air circulation at 40 ± 2°C for about 24 h. Finally, the film samples were removed from plates.

The tensile strength and elongation of CF were measured by a Texture Analyzer (Stable Micro Systems, TA–XT–2i, UK) with a 50-N load cell. The testing speed for texture analysis was 2 mm s^{-1}. The thickness was measured by a digital micrometer (Insize, IP54, Brazil) with 0.0010 mm of resolution [23].

2.2. Adsorption experiments

The vanadium stock solution (1.0 g L^{-1}) was prepared using NH_4VO_3 (purity of 99.0%) (Merck, Germany), and all the assays were carried out by diluting this solution. The pH was adjusted using buffer disodium phosphate/citric acid solution 0.1 mol L^{-1}, and it was measured by a pH meter (Mars, MB10, Brazil). In all the assays, the CF were divided in portions with size of 1 cm × 1 cm.

The adsorption tests were carried out in two steps: RSM experiments and equilibrium experiments. For the RSM experiments, the initial vanadium concentration was 200 mg L^{-1} and the effects of the pH (4, 6, and 8) and the CF dosage (100, 300, and 500 mg L^{-1}) were evaluated. The flasks were agitated at 100 rpm and 333 K using thermostatic agitator—Wagner type (Fanem, 315 SE, Brazil) for 24 h. In the equilibrium experiments, the pH and the CF dosage were fixed (according to the RSM results) and the initial vanadium concentration ranged from 25 to 400 mg L^{-1}. The flasks were agitated at 100 rpm (Fanem, 315 SE, Brazil) under different temperatures (293, 313, and 333 K) until equilibrium. The remaining vanadium concentration was measured by atomic absorption spectrometry with flame (GBC Avanta, 932AA, Australia). The assays were performed in replicate ($n = 3$) and the blank tests were realized. The removal percentage (R), the adsorption capacity (q), and the equilibrium adsorption capacity (q_e) were determined by Eqs. (1)–(3):

$$R = \frac{(C_0 - C_e)}{C_0} \times 100 \quad (1)$$

$$q = \frac{V(C_0 - C_f)}{m} \quad (2)$$

$$q_e = \frac{V(C_0 - C_e)}{m} \quad (3)$$

where C_0 is the initial vanadium concentration in liquid phase (mg L^{-1}), C_e is the equilibrium vanadium concentration in liquid phase (mg L^{-1}), C_f is the final vanadium concentration in liquid phase (mg L^{-1}), m is the amount of CF (g), and V is the volume of solution (L).

2.3. Response surface methodology

The adsorption of heavy metals is influenced by various experimental parameters, such as pH, temperature, stirring rate, initial concentration, amount of adsorbent, and contact time [12,13,18,24]. To evaluate these effects, RSM is a good statistical method [3,25]. In this work, RSM was utilized for the optimization the vanadium adsorption onto CF as a function of pH and CF dosage [25]. The results were the vanadium removal percentage (R) and the adsorption capacity (q). The levels and factors were selected by preliminary test and literature [18,19,26], and are shown in Table 1.

The vanadium removal percentage (R) and adsorption capacity (q) were represented as a function of independent variables according to Eq. (4):

$$Y = a + \sum_{i=1}^{n} b_i x_i + \sum_{i=1}^{n} b_{ii} x_i^2 + \sum_{i=1}^{n-1} \sum_{j=i+1}^{n} b_{ij} x_i x_j \quad (4)$$

where Y is the predicted response (R or q), a is the constant coefficient, b_i is the linear coefficients, b_{ij} is the interaction coefficients, b_{ii} is the quadratic coefficients, and x_i and x_j are the coded values of the variables.

The second-order model (Eq. (4)) was evaluated by Fischer's test, and the proportion of variance explained from the model was given by the multiple coefficient of determination, R^2. The significance level was 95% ($p < 0.05$), and the non–significant factors were excluded [25]. The results were analyzed by Statistic version 7.0 (StatSoft Inc., USA) software.

2.4. Adsorption analysis by equilibrium and thermodynamic data

Adsorption isotherm models are widely used to describe the adsorption process and investigate equilibrium and thermodynamics of adsorption [5,27]. In this work, the equilibrium data were obtained at 293, 313, and 333 K, and the curves were fitted with the Freundlich and Brunauer–Emmett–Teller (BET) isotherm models.

The Freundlich model assumes that the adsorption surface is heterogeneous and it can be represented by Eq. (5) [28]:

$$q_e = k_F C_e^{1/n} \quad (5)$$

where k_F is the Freundlich constant ((mg g^{-1}) (mg $L^{-1})^{-1/n}$) and $1/n$ is the heterogeneity factor.

The BET isotherm is an extension of the Langmuir theory for monolayer adsorption to multilayer adsorption, when the increase of adsorbate–adsorbate interaction and multilayer formation occurs due to secondary adsorption at a given site and it can be represented by Eq. (6) [29]:

$$q_e = \frac{q_{BET} K_1 C_e}{(1 - K_2 C_e)(1 - K_2 C_e + K_1 C_e)} \quad (6)$$

where q_{BET} is the monolayer adsorption capacity (mg g^{-1}), K_1 and K_2 are the BET constants (L mg^{-1}). The equilibrium parameters were determined by

Table 1
Experimental design matrix and results for the vanadium adsorption onto CF

Experiment (n°)	pH [coded form]	CF dosage (mg L^{-1}) [coded form]	R (%)[a]	q (mg g^{-1})[a]
1	4 [−1]	100 [−1]	23.4 ± 0.4	233.6 ± 0.2
2	4 [−1]	300 [0]	33.3 ± 0.3	110.9 ± 0.1
3	4 [−1]	500 [+1]	38.9 ± 0.1	77.9 ± 0.2
4	6 [0]	100 [−1]	25.1 ± 0.1	251.4 ± 0.3
5	6 [0]	300 [0]	50.3 ± 0.2	167.2 ± 0.7
6	6 [0]	500 [+1]	39.9 ± 0.6	79.9 ± 0.3
7	8 [+1]	100 [−1]	18.0 ± 0.2	180.1 ± 0.5
8	8 [+1]	300 [0]	19.7 ± 0.3	65.8 ± 0.1
9	8 [+1]	500 [+1]	20.0 ± 0.2	40.0 ± 0.6

Note: R: vanadium removal percentage; q: adsorption capacity.
[a]Mean ± standard deviation (n = 3).

nonlinear regression, using Statistic 7.0 software (Statsoft, USA). Coefficient of determination (R^2) and average relative error (ARE) were used to select the best fit isotherm model.

The Gibb's free energy (ΔG°), for the adsorption of vanadium by CF was determined by Eq. (7) [30]:

$$\Delta G^\circ = -RT \ln(\rho_w K_D) \quad (7)$$

where K_D is the thermodynamic equilibrium constant (L mol^{-1}), ρ_w is the water density (g L^{-1}), T is the temperature (K), and R is the universal gas constant (8.314 J mol^{-1} K^{-1}). The K_D values were estimated from the slope of initial linear portion of q_e vs. C_e [31].

The enthalpy change (ΔH°) (kJ mol^{-1}) and entropy change (ΔS°) (kJ mol^{-1} K^{-1}) were determined by van't Hoff's plot, according to Eq. (8) [30–32]:

$$\ln(\rho_w K_D) = \frac{\Delta S^\circ}{R} - \frac{\Delta H^\circ}{RT} \quad (8)$$

2.5. Evaluation of CF–vanadium interactions

In order to evaluate the CF–vanadium interactions, the CF were analyzed by FTIR and TGA before and after the adsorption process. The identification and possible alterations of the functional groups were carried out using infrared analysis with attenuated total reflectance (FTIR–ATR) (Prestige 21, the 210045, Japan). The TGA was also performed with a heating rate of 10°C min^{-1}, in the temperature range from 20 to 500°C under N_2 at 50 mL min^{-1} (Shimadzu, DTG–60, Japan).

3. Results and discussion

3.1. CF characteristics

The CF were characterized according to the tensile strength, elongation, and thickness. The values were for tensile strength of 27.6 ± 2.3 MPa and elongation of 12.6 ± 1.3%. The CF thickness was of 62 ± 4 μm. It was also observed that CF maintained its physical structure after adsorption process. Based on these results and on the literature [9,12], it can be affirmed that CF have good mechanical properties and are suitable for use in adsorption processes. These characteristics can facilitate the phase separation and regeneration after adsorption process [13].

3.2. Optimization by RSM

The vanadium adsorption onto CF was optimized as a function of pH and CF dosage by RSM. The factors, levels, and experimental results for removal percentage (R) and adsorption capacity (q) are shown in Table 1. Analysis of variance (ANOVA) was employed in order to verify the significance of pH and CF dosage on the responses (R and q). The ANOVA showed that the linear and quadratic effects of pH and CF dosage were significant ($p < 0.05$) in relation to R and q. The interaction effect was also significant ($p < 0.05$). The statistical polynomial quadratic models which represent the dependence of vanadium removal percentage (R) and adsorption capacity (q) in relation to the pH (coded form: x_1) and the CF dosage (coded form: x_2) are shown by Eqs. (9) and (10), respectively:

$$R = 44.8 - 2.8x_1 + 1.9x_2 - 15.7x_1^2 - 9.8x_2^2 + 1.8x_1x_2 \quad (9)$$

$$q = 146.9 - 22.8x_1 - 77.9x_2 - 48.2x_1^2 + 29.1x_2^2 + 4.0x_1x_2 \quad (10)$$

In order to verify the prediction and significance of the statistical models (Eqs. (9) and (10)), ANOVA and Fischer's F test were employed. The high values of coefficients of determination ($R^2 = 0.97$ and 0.98, respectively) showed that the models were significant. The calculated F values ($F_{CALC} = 13.3$ and 95.2) were higher than standard F values ($F_{TAB} = 3.11$) showing that the models were predictive. It was also verified that the distribution of residues was random around zero, for both responses. Then, the statistical models were used to generate the response surfaces (Fig. 1(a) and (b)), which represents the R and q as a function of independent variables.

Fig. 1(a) and (b) shows that the vanadium removal percentage (R) and adsorption capacity (q) showed a parabolic behavior in relation to the pH, being the maximum values obtained at pH 6. This behavior can be explained due to the CF and vanadium characteristics under different pH values. In the acidic region (pH 4 and 6), the amino groups of CF are protonated, but in the alkaline region (pH 8), a decrease in these positive charges occurs [9]. The forms of vanadium existing in aqueous solution depend on its concentration and the pH value. The vanadium in the pH values of 4, 6, and 8 are mainly in the forms of $HV_{10}O_{28}^{5-}$, $V_{10}O_{28}^{6-}$, and $V_4O_{12}^{4-}$, respectively [26]. Thus, the $V_{10}O_{28}^{6-}$ can be preferentially adsorbed due to the highest electrostatic interaction with the protonated adsorbent.

Fig. 1(a) shows that the increase in CF dosage (from 100 to 300 mg L^{-1}) led to a strong increase in the vanadium removal percentage. This occurred

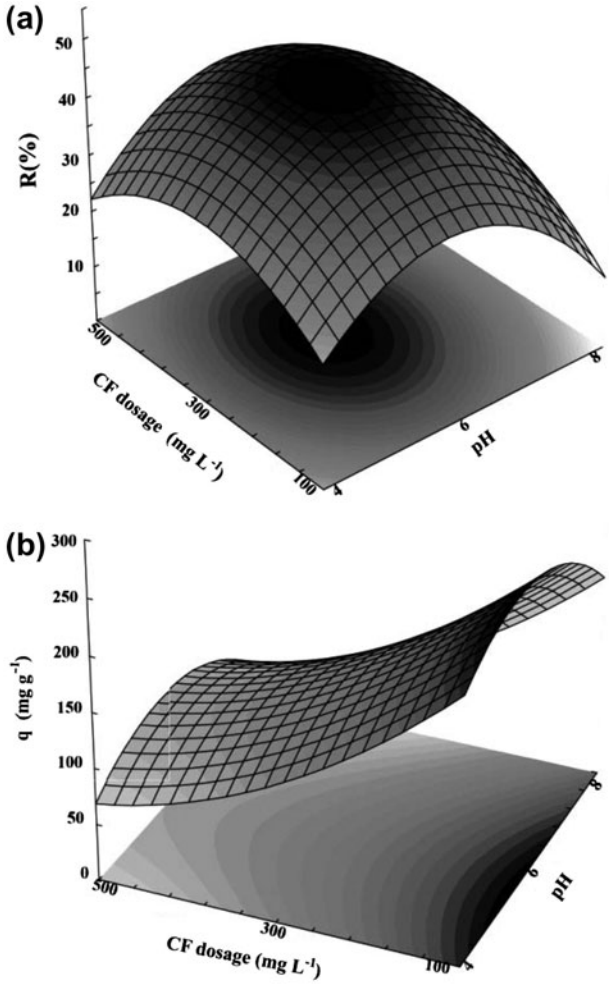

Fig. 1. Experimental design results R (a) and q (b) as a function of independent variables.

because high CF dosage in the solution provides more available sites for the vanadium adsorption. However, when the CF dosage increased to 500 mg L^{-1}, a smaller variation in the removal percentage was observed. Aydin and Aksoy [33] found similar results in the chromium adsorption onto chitosan. Otherwise, the Fig. 1(b) shows that adsorption capacity increased when the CF dosage decreased. This behavior can be justified because the adsorption capacity was inversely proportional to the amount of CF (see Eq. (2)).

In the considered range of the present work, the more suitable conditions for the vanadium adsorption onto CF were found in the maximum points of the response surface curves (Fig. 1(a) and (b)). These conditions were in pH 6.0 and CF dosages of 300 and 100 g L^{-1}, respectively, for the removal percentage ($R = 50.3\%$) and the adsorption capacity ($q = 251.4$ mg g^{-1}). Guzmán et al. [16], in the vanadium adsorption onto chitosan powder, obtained values of 390.9 mg g^{-1} at pH 5.2. Bhatnagar et al. [34] found values of 27.0 mg g^{-1}, in the vanadium adsorption onto waste metal sludge. Table 2 shows a comparison of CF with other adsorbents for vanadium removal from aqueous solution. In this table, it is observed that CF presented suitable adsorption capacities, and it can be used as an adsorbent to remove vanadium from aqueous solutions [16,34,35].

3.3. Equilibrium and thermodynamic results

The equilibrium isotherms were performed at pH 6 and CF dosage of 300 mg L^{-1} (based on the results of Section 3.2). Fig. 2 shows the equilibrium curves of vanadium adsorption onto CF under different temperatures (293, 313, and 333 K). Based on Ruthven [36], it can be inferred that the isotherms of vanadium adsorption onto CF were type II (Fig. 2). This shape is generally observed in adsorbents with a wide range of pore sizes. In this case, there is a continuous progression with increasing loading from monolayer to multilayer [5]. Fig. 2 shows that the increase in temperature led to an increase in the vanadium adsorption capacity. This behavior can be attributed to the increase in the vanadium mobility in the solution [34]. Furthermore, the increase in temperature also caused a strong swelling effect within the internal structure of the CF [9], which facilitated the vanadium penetration.

Freundlich and BET isotherm models were used to fit the equilibrium data of vanadium adsorption onto CF at different temperatures. The isotherm parameters are shown in Table 3. Based on results of R^2 and ARE,

Table 2
Experimental results in similar studies relatives to vanadium adsorption

Adsorbent	Adsorbent dosage (mg L^{-1})	pH	Adsorption capacity	Refs.
Chitosan films (CF)	300	6	251.4	[This work]
Chitosan flakes	250	3	449.5	[16]
Metal sludge	2,000	7.6	27	[34]
Chitosan–zirconium(IV) composite	100	4	208	[35]

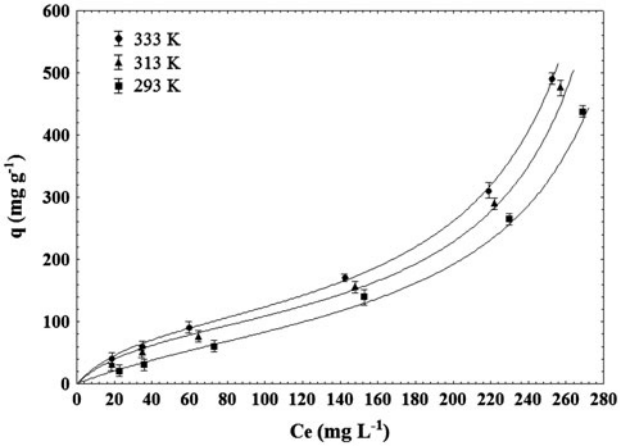

Fig. 2. Equilibrium experimental data.

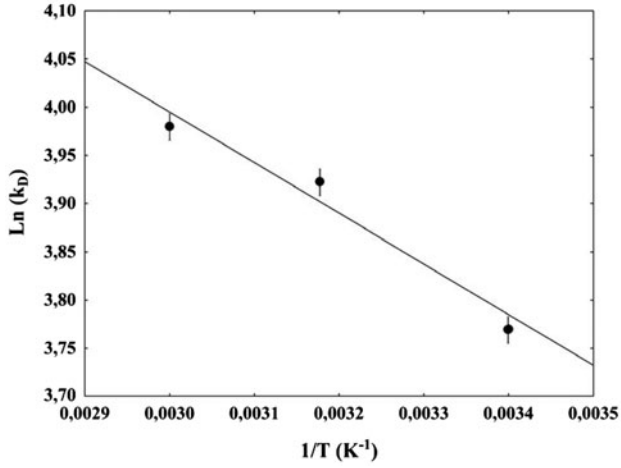

Fig. 3. van't Hoff plot.

Table 3
Isotherm parameters for the vanadium adsorption onto CF

Model	293 K	313 K	333 K
Freundlich			
k_F (mg g^{-1}) (L $mg^{-1})^{-1/n}$	0.031 ± 0.2	1.401 ± 0.1	0.549 ± 0.2
n	0.592 ± 0.4	0.939 ± 0.3	0.833 ± 0.1
R^2	0.939	0.900	0.914
ARE (%)	13.73	13.30	14.29
BET			
K_1 (L mg^{-1})	0.013 ± 0.1	0.032 ± 0.3	0.033 ± 0.2
$K_2 \times 10^3$ (L mg^{-1})	2.97 ± 0.5	3.12 ± 0.4	3.15 ± 0.4
q_{BET} (mg g^{-1})	90.13 ± 0.4	90.90 ± 0.1	102.25 ± 0.5
R^2	0.985	0.982	0.971
ARE (%)	8.32	8.21	9.01

Table 4
Thermodynamic parameters for the vanadium adsorption onto CF

Temperature (K)	ΔG° (kJ $mol^{-1})^a$	ΔH° (kJ $mol^{-1})^a$	ΔS° (kJ mol^{-1} $K^{-1})^a$
293	−16.44 ± 0.01	9.02 ± 0.10	0.09 ± 0.01
313	−18.45 ± 0.01		
333	−20.07 ± 0.02		

[a]Mean ± standard deviation (n = 3).

it can be affirmed that the BET isotherm model was the more appropriate to fit the experimental data. This suggests a multilayer adsorption and corroborates with the isotherm shape. Piccin et al. [37] in the adsorption of black 210 dye on tannery solid waste verified that the BET model was the more adequate. They attributed this behavior due to the secondary adsorption at a given site, forming a multilayer and hence leading to a satisfactory adjustment to the BET model. The K_1 and K_2 values increased with the temperature confirming that the adsorption was favored at 333 K (Table 3). K_1 represents the inverse of the equilibrium concentration in the liquid when the adsorption capacity reaches half the monolayer adsorption capacity. The K_2 values represent the inverse of the concentration value when the isotherm becomes a vertical line, and they are associated with superficial solubility of ions [37]. Furthermore, the increase in temperature caused an increase in the q_{BET} value from 90.9 to 102.3 mg g^{-1}.

The van't Hoff plot and the thermodynamic parameters are shown in Fig. 3 and Table 4, respectively. The R^2 value of the linear fit was of 0.9892. In Table 4, the negative ΔG° values indicate that the adsorption process was favorable and spontaneous. The positive ΔH° value showed that the vanadium adsorption onto CF was an endothermic process [38,39].

The magnitude of ΔH° suggested that physical sorption mechanisms were involved in vanadium adsorption onto CF [39]. The positive ΔS° value suggested that increased randomness at the solid–solution interface occurred in the internal structure due to the uptake of vanadium onto CF [40,41].

3.4. CF–vanadium interactions

The possible CF–vanadium interactions were elucidated using FTIR and TGA. Fig. 4 shows the CF vibrational spectrum before and after the adsorption. Fig. 4(a) shows the characteristic bands of CF, relative

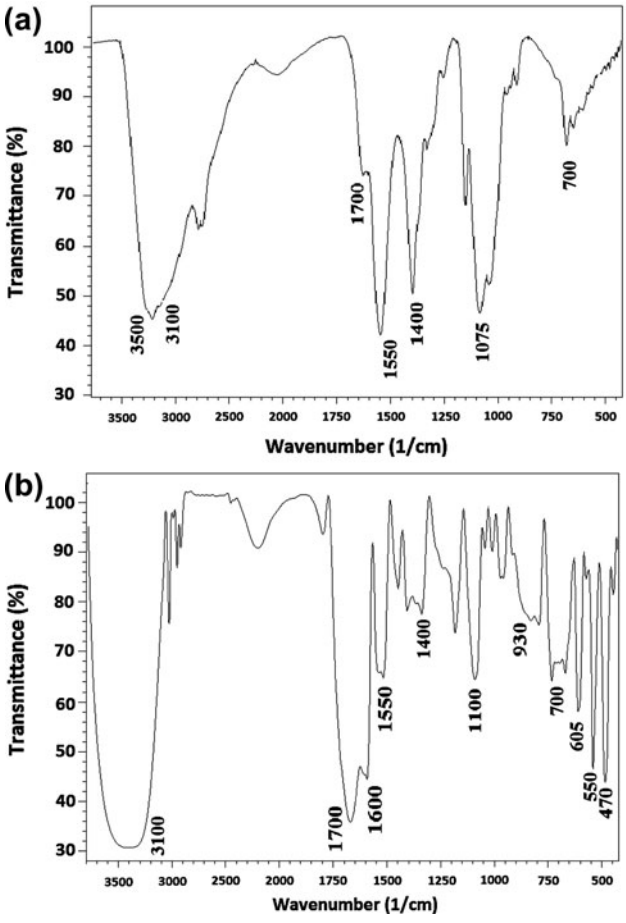

Fig. 4. CF vibrational spectrum before (a) and after (b) the adsorption.

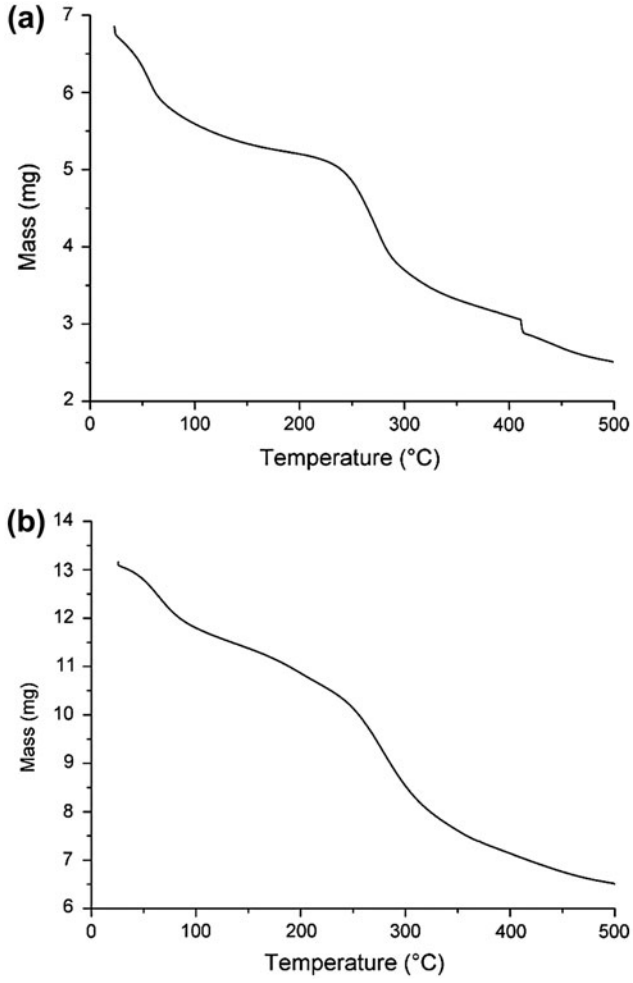

Fig. 5. TGA curves of CF before (a) and after adsorption (b).

to the N–H and O–H stretching between 3,100 and 3,500 cm^{-1}, respectively, and the C–N in 1,550 and 1,075 cm^{-1} [7], respectively.

After the adsorption process (Fig. 4(b)), shifts occurred in the CF amino and hydroxyl groups and a new absorption appears at 930 cm^{-1} (unsymmetrical) due to the stretching frequency of the V=O group [42]. This is due to partially superposed absorptions of different vanadium sites. Furthermore, a series of bands resulting from V–O sensitive modes between 450 and 600 cm^{-1} were present in the spectrum and indicate that there are vanadium ions in different points in the CF.

Fig. 5 shows the TGA curves of CF before adsorption process (Fig. 5(a)) and after adsorption process (Fig. 5(b)). In both the cases, CF showed three weight loss steps. The first step, below 110˚C, can be ascribed to the evaporation of adsorbed water molecules. Then, the slight weight loss from 110 to 260˚C can be assigned to the removal of the labile oxygen-containing functional groups, like CO, CO_2, and H_2O. The last weight loss, in the range from 260 to 500˚C, can be assigned to the carbon skeleton decomposition of CF [43,44]. However, after the adsorption process (Fig. 5(b)), a higher amount of sample remained (see at the end of TGA curve). This mass can be attributed to the adsorbed vanadium, whose melting point is around 1,910˚C [45]. FTIR and TGA confirmed the vanadium adsorption on CF.

3.5. Desorption and recycling

In order to verify the possible reuse of CF, adsorption–desorption cycles were carried out using 100 mL of eluent solution and 50 mg of CF loaded with vanadium. NH_4Cl solution (0.01 mol L^{-1}) was used as eluent. It was found that all vanadium was removed from the CF during six adsorption–desorption cycles.

Table 5
Characteristics of CF after all regeneration cycles

Characteristics[b]	Cycle	1°	2°	3°	4°	5°	6°
Mechanical properties	Tensile strength (MPa)	29.1 ± 3.1[a]	28.9 ± 2.3[a]	29.3 ± 2.1[a]	28.8 ± 2.5[a]	28.2 ± 1.1[a]	27.9 ± 3.1[a]
	Elongation (%)	7.5 ± 0.5[a]	7.4 ± 0.1[a]	7.5 ± 0.3[a]	7.3 ± 0.2[a]	7.4 ± 0.4[a]	7.4 ± 0.2[a]
	Thickness (μm)	61 ± 4[a]	62 ± 3[a]	61 ± 5[a]	61 ± 4[a]	61 ± 3[a]	61 ± 5[a]

Note: Equal letters in the same line were not significantly different ($p > 0.05$).
[a]The significance level is of 95%.
[b]Mean ± standard deviation ($n = 3$).

This result suggests the electrostatic interaction between CF and vanadium [18]. Six adsorption–desorption cycles were possible, maintaining similar behavior to the adsorption capacities (around 250 mg g^{-1}) and mechanical properties of CF. Table 5 shows the characteristics of CF during all regeneration cycles.

4. Conclusions

The vanadium removal from aqueous solutions by adsorption onto CF was studied. CF showed good mechanical properties (tensile strength and elongation), which facilitated the phase separation after adsorption. RSM showed that the more suitable adsorption conditions were in pH 6 and CF dosages of 100 and 300 mg L^{-1} for removal percentage and adsorption capacity, respectively. The values of vanadium removal percentage and adsorption capacity obtained under these conditions were 50.3% and 251.4 mg g^{-1}, respectively. The BET model presented best fit with the equilibrium experimental data, suggesting a multilayer adsorption. The thermodynamic study demonstrated that the adsorption process was spontaneous, favorable, and endothermic. FTIR and TGA analysis confirmed the presence of vanadium in the CF. Practically, all vanadium was removed from the CF during six adsorption–desorption cycles.

Acknowledgment

The authors would like to thank CAPES (Brazilian Agency for Improvement of Graduate Personnel) and CNPq (National Council of Science and Technological Development) for the financial support.

References

[1] S.A. Baig, Q. Wang, X. Lv, X. Xu, Removal of hexavalent chromium by limonite in aqueous solutions, Hydrometallurgy 138 (2013) 33–39.
[2] X.S. Wang, F. Liu, H.J. Lu, P. Zhang, H.Y. Zhou, Adsorption kinetics of Cd(II) from aqueous solution by magnetite, Desalin. Water Treat. 36 (2011) 203–209.
[3] G.L. Dotto, T.R.S. Cadaval, L.A.A. Pinto, Preparation of bionanoparticles derived from *Spirulina platensis* and its application for Cr(VI) removal from aqueous solutions, J. Ind. Eng. Chem. 18 (2012) 1925–1930.
[4] L.V.A. Gurgel, L.F. Gil, Adsorption of Cu(II), Cd(II) and Pb(II) from aqueous single metal solutions by succinylated twice–mercerized sugarcane bagasse functionalized with triethylenetetramine, Water Res. 43 (2009) 4479–4488.
[5] G. Blázquez, M. Calero, F. Hernáinz, G. Tenorio, M.A. Martín-Lara, Equilibrium biosorption of lead(II) from aqueous solutions by solid waste from olive–oil production, Chem. Eng. J. 160 (2010) 615–622.
[6] N.S. Barot, H.K. Bagla, Eco-friendly waste water treatment by cow dung powder (Adsorption studies of Cr(III), Cr(VI) and Cd(II) using tracer technique), Desalin. Water Treat. 38 (2012) 104–113.
[7] T.R.S. Cadaval Jr., A.S. Camara, G.L. Dotto, L.A.A. Pinto, Adsorption of Cr(VI) by chitosan with different deacetylationdegrees, Desalin. Water Treat. 51 (2013) 7690–7699.
[8] G.L. Dotto, L.A.A. Pinto, Adsorption of food dyes acid blue 9 and food yellow 3 onto chitosan: Stirring rate effect in kinetics and mechanism, J. Hazard. Mater. 187 (2011) 164–170.
[9] G.L. Dotto, J.M. Moura, T.R.S. Cadaval, L.A.A. Pinto, Application of chitosan films for the removal of food dyes from aqueous solutions by adsorption, Chem. Eng. J. 214 (2013) 8–16.
[10] Y. Tao, L. Ye, J. Pan, Y. Wang, B. Tang, Removal of Pb(II) from aqueous solution on chitosan/TiO_2 hybrid film, J. Hazard. Mater. 161 (2009) 718–722.
[11] A.C.L. Batista, E.R. Villanueva, R.V.S. Amorim, M.T. Tavares, G.M. Campos-Takaki, Chromium(VI) ion adsorption features of chitosan film and its chitosan/zeolite conjugate 13X film, Molecules 16 (2011) 3569–3579.
[12] R.S. Vieira, M.L.M. Oliveira, E. Guibal, E. Rodríguez-Castellón, M.M. Beppu, Copper, mercury and chromium adsorption on natural and crosslinked chitosan films: An XPS investigation of mechanism, Colloids Surf., A Physicochem. Eng. Aspects 374 (2011) 108–114.
[13] A.R. Fajardo, L.C. Lopes, A.F. Rubira, E.C. Muniz, Development and application of chitosan/poly(vinyl alcohol) films for removal and recovery of Pb(II), Chem. Eng. J. 183 (2012) 253–260.

[14] F.M. Al–Kharafi, W.A. Badawy, Electrochemical behavior of vanadium in aqueous solutions of different pH, Electrochim. Acta 42 (1997) 579–586.
[15] W. Zubot, M.D. MacKinnon, P. Chelme-Ayala, D.W. Smith, M.G. El-Din, Petroleum coke adsorption as a water management option for oil sands process-affected water, Sci. Total Environ. 427–428 (2012) 364–372.
[16] J. Guzmán, I. Saucedo, R. Navarro, J. Revilla, E. Guibal, Vanadium interactions with chitosan: Influence of polymer protonation and metal speciation, Langmuir 18 (2002) 1567–1573.
[17] B. Gummow, Vanadium: Environmental Pollution and Health Effects, Elsevier, Amsterdam, 2011.
[18] E. Guibal, Interactions of metal ions with chitosan-based sorbents: A review, Sep. Purif. Technol. 38 (2004) 43–74.
[19] G. Crini, P.M. Badot, Application of chitosan, a natural aminopolysaccharide, for dye removal from aqueous solutions by adsorption processes using batch studies: A review of recent literature, Prog. Polym. Sci. 33 (2008) 399–447.
[20] R.F. Weska, J.M. Moura, L.M. Batista, J. Rizzi, L.A.A. Pinto, Optimization of deacetylation in the production of chitosan from shrimp wastes: Use of response surface methodology, J. Food Eng. 80 (2007) 749–753.
[21] C.M. Moura, J.M. Moura, N.M. Soares, L.A.A. Pinto, Evaluation of molar weight and deacetylation degree of chitosan during chitin deacetylation reaction: Used to produce biofilm, Chem. Eng. Process. Process Intensif. 50 (2011) 351–355.
[22] G.L. Dotto, V.C. Souza, J.M. Moura, C.M. Moura, L.A.A. Pinto, Influence of drying techniques on the characteristics of chitosan and the quality of biopolymer films, Drying Technol. 29 (2011) 1784–1791.
[23] American Society for Testing and Materials (ASTM), Standard test Methods for Tensile Properties of Thin Plastic Sheeting (Standard D882–02, 162–170), Philadelphia, PA, 2001.
[24] W. Wainipee, D.J. Weiss, M.A. Sephton, B.J. Coles, C. Unsworth, R. Court, The effect of crude oil on arsenate adsorption on goethite, Water Res. 44 (2010) 5673–5683.
[25] R.H. Myers, D.C. Montgomery, Response Surface Methodology: Process and Product Optimization using Designed Experiments, John Wiley & Sons, New York, NY, 2002.
[26] Y. Fan, X. Wang, M. Wang, Separation and recovery of chromium and vanadium from vanadium-containing chromate solution by ion exchange, Hydrometallurgy 136 (2013) 31–35.
[27] M.I. El–Khaiary, G.F. Malash, Common data analysis errors in batch adsorption studies, Hydrometallurgy 105 (2011) 314–320.
[28] W. Li, L. Qi, W. Aiqin, Adsorption of cationic dye on N,O-carboxymethylchitosan from aqueous solutions: Equilibrium, kinetics, and adsorption mechanism, Polym. Bull. 65 (2010) 961–975.
[29] A. Ebadi, J.S. Soltan Mohammadzadeh, A. Khudiev, What is the correct form of BET isotherm for modeling liquid phase adsorption? Adsorption 15 (2009) 65–73.
[30] K.S. Tapan, FMMdK Subarna, Adsorption behavior of [meso-tetrakis (4-carboxylatophenyl) porphyrinato] oxovanadium(IV) tetrasodium in aqueous solution onto chitosan, Polym. Bull. 70 (2013) 2047–2063.
[31] S.K. Milonjic, A consideration of the correct calculation of thermodynamic parameters of adsorption, J. Serb. Chem. Soc. 72 (2007) 1363–1367.
[32] S. Dawood, T.K. Sen, Removal of anionic dye Congo red from aqueous solution by raw pine and acid–treated pine cone powder as adsorbent: Equilibrium, thermodynamic, kinetics, mechanism and process design, Water Res. 46 (2012) 1933–1946.
[33] Y.A. Aydın, N.D. Aksoy, Adsorption of chromium on chitosan: Optimization, kinetics and thermodynamics, Chem. Eng. J. 151 (2009) 188–194.
[34] A. Bhatnagar, A.K. Minocha, D. Pudasainee, H.K. Chung, S.H. Kim, H.S. Kim, G. Lee, B. Min, B.H. Jeon, Vanadium removal from water by waste metal sludge and cement immobilization, Chem. Eng. J. 144 (2008) 197–204.
[35] Z. Lingfan, L. Xin, X. Wei, Z. Wenqing, Preparation and characterization of chitosan–zirconium(IV) composite for adsorption of vanadium(V), Int. J. Biol. Macromol. 64 (2014) 155–161.
[36] D.M. Ruthven, Principles of Adsorption and Adsorption Process, John Wiley & Sons, New York, NY, 1984.
[37] J.S. Piccin, L.A. Feris, M. Cooper, M. Gutterres, Dye adsorption by leather waste: Mechanism diffusion, nature studies, and thermodynamic data, J. Chem. Eng. Data 58 (2013) 873–882.
[38] Y. Guide, T. Lin, L. Xiaoxia, Z. Guangming, C. Ye, W. Xue, Z. Yaoyu, L. Sisi, F. Yan, Z. Yi, Cd(II) removal from aqueous solution by adsorption on α-ketoglutaricacid-modified magnetic chitosan, Appl. Surf. Sci. 292 (2014) 710–716.
[39] C.L. Sun, C.S. Wang, Estimation on the intramolecular hydrogen-bonding energies in proteins and peptides by the analytic potential energy function, J. Mol. Struct. Theochem. 956 (2010) 38–43.
[40] Y. Guide, T. Lin, Z. Guangming, C. Ye, T. Jing, P. Ya, Z. Yaoyu, L. Yuanyuan, W. Jiajia, Z. Sheng, X. Weiping, Simultaneous removal of lead and phenol contamination from water by nitrogen-functionalized magnetic ordered mesoporous carbon, Chem. Eng. J. 259 (2015) 854–864.
[41] N.F. Cardoso, E.C. Lima, B. Royer, M.V. Bach, G.L. Dotto, L.A.A. Pinto, T. Calvete, Comparison of *Spirulina platensis* microalgae and commercial activated carbon as adsorbents for the removal of Reactive Red 120 dye from aqueous effluents, J. Hazard. Mater. 241–242 (2012) 146–153.
[42] P.A.M. Williams, E.J. Baran, Spectroscopic investigation of the VO_2^+/hyaluronate interaction, Carbohydr. Polym. 86 (2011) 1385–1388.
[43] C.M. Futalan, C.C. Kan, M.L. Dalida, K.J. Hsien, C. Pascua, M.W. Wan, Comparative and competitive adsorption of copper, lead and nickel using chitosan immobilized on bentonite, Carbohydr. Polym. 83 (2011) 528–536.
[44] A.P. Martínez-Camacho, M.O. Cortez-Rocha, J.M. Ezquerra-Brauer, A.Z. Graciano-Verdugo, F. Rodriguez-Félix, M.M. Castillo-Ortega, M.S. Yépiz-Gómez, M. Plascencia-Jatomea, Chitosan composite films: Thermal, structural, mechanical and antifungal properties, Carbohydr. Polym. 82 (2010) 305–315.
[45] R.H. Perry, D.W. Green, Perry's Chemical Engineers' Handbook, seventh ed., McGraw–Hill, New York, 1997.